CRREL
REPORT 87-17

US Army Corps of Engineers
Cold Regions Research & Engineering Laboratory

Evaluation of the magnetic induction conductivity method for detecting frazil ice deposits

CRREL Report 87-17

September 1987

Evaluation of the magnetic induction conductivity method for detecting frazil ice deposits

Steven A. Arcone, Bruce E. Brockett, Daniel E. Lawson
and Edward F. Chacho, Jr.

Prepared for
OFFICE OF THE CHIEF OF ENGINEERS

Unclassified
SECURITY CLASSIFICATION OF THIS PAGE

REPORT DOCUMENTATION PAGE

Form Approved
OMB No 0704-0188
Exp. Date: Jun 30, 1986

1a. REPORT SECURITY CLASSIFICATION Unclassified	1b. RESTRICTIVE MARKINGS
2a. SECURITY CLASSIFICATION AUTHORITY	3. DISTRIBUTION/AVAILABILITY OF REPORT Approved for public release; distribution is unlimited.
2b. DECLASSIFICATION/DOWNGRADING SCHEDULE	
4. PERFORMING ORGANIZATION REPORT NUMBER(S) CRREL Report 87-17	5. MONITORING ORGANIZATION REPORT NUMBER(S)
6a. NAME OF PERFORMING ORGANIZATION U.S. Army Cold Regions Research and Engineering Laboratory 6b. OFFICE SYMBOL (*If applicable*) CECRL	7a. NAME OF MONITORING ORGANIZATION Office of the Chief of Engineers
6c. ADDRESS (*City, State, and ZIP Code*) Hanover, New Hampshire 03755-1290	7b. ADDRESS (*City, State, and ZIP Code*) Washington, D.C. 20314-1000
8a. NAME OF FUNDING/SPONSORING ORGANIZATION 8b. OFFICE SYMBOL (*If applicable*)	9. PROCUREMENT INSTRUMENT IDENTIFICATION NUMBER CWIS 31722
8c. ADDRESS (*City, State, and ZIP Code*)	10. SOURCE OF FUNDING NUMBERS PROGRAM ELEMENT NO. / PROJECT NO. 4A1611 02AT24 / TASK NO. SS / WORK UNIT ACCESSION NO. 014

11. TITLE (*Include Security Classification*)
Evaluation of the Magnetic Induction Conductivity Method for Detecting Frazil Ice Deposits (Unclassified)

12. PERSONAL AUTHOR(S)
Arcone, Steven A.; Brockett, Bruce E.; Lawson, Daniel E.; and Chacho, Edward F. Jr.

13a. TYPE OF REPORT	13b. TIME COVERED	14. DATE OF REPORT (*Year, Month, Day*)	15. PAGE COUNT
	FROM _____ TO _____	September 1987	17

16. SUPPLEMENTARY NOTATION

17. COSATI CODES			18. SUBJECT TERMS (*Continue on reverse if necessary and identify by block number*)
FIELD	GROUP	SUB-GROUP	Frazil ice Magnetic induction Resistivity surveying

19. ABSTRACT (*Continue on reverse if necessary and identify by block number*)

The ability to map frazil ice deposits and water channels beneath an ice-covered river in central Alaska using the magnetic induction conductivity (MI) technique has been assessed. The study was performed during the first week of March 1986 on the Tanana River near Fairbanks and employed a commercially available instrument operating at a fixed frequency with a fixed antenna (coil) spacing and orientation. Comparisons of the MI data with theoretical models based upon physical data measured along three cross sections of the river demonstrate the sensitivity of the MI technique to frazil ice deposits. The conductivity generally derived for the frazil ice deposits encountered is very low ($\sim 6.3 \times 10^{-4}$ S/m) when compared with the measured value for water (~ 0.011 S/m), and is similar to the calculated values for gravel and sandy gravel bed sediments. In all three cross sections, maxima in the apparent conductivity profiles correlated with frazil ice deposits. Difficulties, possibly due to adverse effects of cold weather upon instrument calibration, affected the quantitative performance of the instrument on one cross section, although the interpretation of the data (locations of open channels vs frazil deposits) was qualitatively unaffected.

20. DISTRIBUTION/AVAILABILITY OF ABSTRACT ☒ UNCLASSIFIED/UNLIMITED ☐ SAME AS RPT. ☐ DTIC USERS	21. ABSTRACT SECURITY CLASSIFICATION Unclassified
22a. NAME OF RESPONSIBLE INDIVIDUAL Steven Arcone	22b. TELEPHONE (*Include Area Code*) 603-646-4100 22c. OFFICE SYMBOL CECRL-RS

DD FORM 1473, 84 MAR — 83 APR edition may be used until exhausted. All other editions are obsolete.

SECURITY CLASSIFICATION OF THIS PAGE
Unclassified

PREFACE

This report was prepared by Dr. Steven A. Arcone, Research Geophysicist, Snow and Ice Branch, and Bruce E. Brockett, Physical Science Technician, Dr. Daniel E. Lawson, Research Physical Scientist, and Edward F. Chacho, Jr., Research Civil Engineer, all of the Geological Sciences Branch, Research Division, of the U.S. Army Cold Regions Research and Engineering Laboratory. Funding for this research was provided by the Office, Chief of Engineers, through the Cold Regions Hydrology Program under Civil Works Unit CWIS 31722 and through DA Project 4A161102AT24, *Research in Snow, Ice and Frozen Ground*; Task SS, *Properties of Cold Regions Materials*; Work Unit 014, *Electromagnetic Characteristics of Snow, Ice, and Frozen Ground.*

The authors thank Allan Delaney of CRREL for his cooperation and valued assistance. Paul Sellmann and Steven Daly of CRREL reviewed this report.

CONTENTS

ILLUSTRATIONS

Figure

Evaluation of the Magnetic Induction Conductivity Method for Detecting Frazil Ice Deposits

STEVEN A. ARCONE, BRUCE E. BROCKETT, DANIEL E. LAWSON
AND EDWARD F. CHACHO, JR.

INTRODUCTION

Frazil ice is the predominant type of ice found in most rivers and streams. Information on frazil ice formation is required to understand the winter hydrology of streams in cold regions as well as to plan navigation routes, design of bridge piers, and for erosion control, water intakes, and pipelines. Frazil dams can form under an ice cover, extend to the river bed, and impede or channel flow. As there may be no or subtle surface manifestations of these frazil deposits, time-consuming drilling is required to locate and map them. Consequently, a remote sensing method was desired to expedite mapping. This paper discusses the use of a magnetic induction technique (MI), which is a noncontact method of measuring ground electrical conductivity.

The initial evaluation of MI for locating frazil ice deposits was undertaken in 1984 as part of a study of the effects of an ice cover on the winter hydrologic regime of the Tanana River near Fairbanks, Alaska (Lawson et al. 1986a). Subice observations through drill holes indicated that extensive deposits of frazil ice tended to channelize flow (Lawson et al. 1986b). During the 1984 studies, both the MI and ground-penetrating radar (GPR) methods (see e.g. Arcone [1985] or Arcone and Delaney [in prep.] for description of GPR in ice surveying) were tested to determine if they could identify the frazil deposits and channels. Extensive data from the access holes were used to evaluate the geophysical data. The results indicated that GPR detection of frazil ice deposits was questionable because: a) the frazil formations were highly reflective due to water content and did not allow penetration (Arcone and Delaney, in prep.), b) the interface between solid frazil deposits and the river bed could not be distinguished, or c) direct coupling between antennas offered too much interference. However, good qualitative correlations were found between the MI response and the presence of open channels and frazil ice deposits.

The objective of this study, therefore, was to assess the ability of the magnetic induction method to map frazil ice deposits in an area of heavy frazil ice accumulation. Three parallel cross sections ranging from 170 to 210 m in length across the Tanana River were profiled for apparent conductivity using MI. The results were compared with apparent conductivity values generated by theoretical models based upon extensive data from drill holes to determine the conductivity of frazil ice and river bottom sediments and the sensitivity of the MI method to frazil ice.

MAGNETIC INDUCTION CONDUCTIVITY METHOD

The MI technique of conductivity mapping utilizes the coupling between two coplanar antenna loops to measure an apparent ground conductivity: apparent in that it is an integration of any inhomogeneities in the ground. A ground-based, portable system has been applied extensively in arctic studies (e.g. Hoekstra 1978, Arcone et al. 1978, 1979) where frozen ground or massive ice formations can offer a noticeable conductivity contrast with the general ground conditions. Its use for measuring sea ice thickness has been reported by Hoekstra et al. (1979) and large-scale airborne systems have also been tried (e.g Fraser 1978).

The MI method derives ground conductivity values from the magnetic field coupling between two loop antennas located at, or slightly above, the earth's surface (Fig. 1). One loop, the transmitter antenna, generates a primary, time-harmonic magnetic field, which couples directly with the

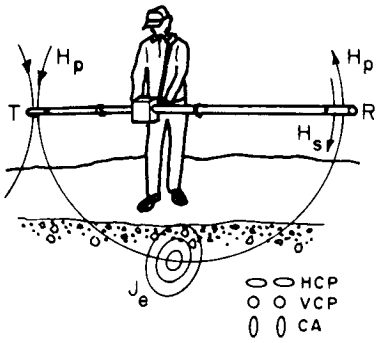

Figure 1. Schematic of the magnetic induction instrument (Geonics EM31) for measuring ground conductivity. The transmitting loop T produces a primary magnetic field H_p (which induces eddy currents J_e within the ground. J_e then produces a secondary magnetic field H_s, which is received out of phase with H_p at the receiver R. The quadrature phase component of H_s/H_p is calibrated in mS/m of conductivity. Also shown are some of the possible loop orientations, two of which—HCP and VCP—are possible with the Geonics EM 31).

receiver loop but also induces electrical currents (sometimes referred to as "eddy" currents) within the ground. These currents then generate a secondary magnetic field, which also couples with the receiver loop. The secondary coupling depends on ground conductivity. The ratio of secondary to primary coupling is usually simply calibrated against conductivity so that this ratio is the quantity measured.

Information about conductivity variations with depth are achieved by varying either the interloop spacing or the loop orientation. Some of the different loop orientations are also shown in Figure 1. They are defined as vertical coplanar (VCP), horizontal coplanar (HCP), and coaxial (CA). Other asymmetric configurations are also possible.

The magnetic coupling is determined from the mutual impedance Z, defined as V/I, where V is the voltage in the transmitter loop and I is the current induced in the receiver loop. Z is determined by the linear combination of primary V_p and secondary V_s coupling such that

$$Z = \frac{V_p + V_s}{I}. \tag{1}$$

Z is normalized by the free space impedance Z_0 (in effect, a measure of the primary coupling), which is determined by the formula (Keller and Frischknecht 1966)

$$Z_0 = \frac{i\mu_0\omega(n_t A_t)(n_r A_r)}{4\pi r^3} \tag{2}$$

where ω = frequency (rad/s)
$\mu_0 = 4\pi \times 10^{-7}$ (Henry/m)
$i = \sqrt{-1}$
n = number of turns
A_t = area of the transmit (t) loop antenna
A_r = area of the receive loop antenna
r = loop separation.

For this study, the Geonics* EM31 was used in the HCP mode. The EM31 uses antenna loops spaced 3.66 m apart and operates at 39 kHz.† These parameters and the normal range of ground conductivity σ (0.1 to 10^{-4} S/m or mhos/m) allow the ratio Z/Z_0 (Keller and Frischknecht 1966, p. 335) to be approximated for HCP antennas lying on homogeneous ground by the formula

$$\frac{Z}{Z_0} = 1 + \left(\frac{\gamma r}{2}\right)^2 \tag{3}$$

because the magnitude of γr is much less than unity. Assuming negligible displacement currents, the quantity γ is related to σ (the inverse of resistivity ϱ) by the formula

$$\gamma = \sqrt{i\omega\mu_0\sigma}, \tag{4}$$

so that eq 3 becomes

$$\frac{Z}{Z_0} = 1 + i\omega\mu_0\sigma r/4. \tag{5}$$

The real part is known as the in-phase component and the imaginary part as the quadrature phase component of the normalized mutual impedance. The EM31 was used only in the quadrature mode for this study.

When the earth is layered, an apparent conductivity σ_a is then defined. This quantity is equal to the conductivity that would produce the same modulus for the mutual impedance above a homogeneous earth. Interpolation curves or computational integrations of integral equations (Keller and Frischknecht 1966, Sinha 1976) must then be used to resolve the different layer resistivities and thicknesses. We used interpretation formulas pub-

* Geonics Ltd., Mississauga, Ontario.
† Most models operate at 10 kHz.

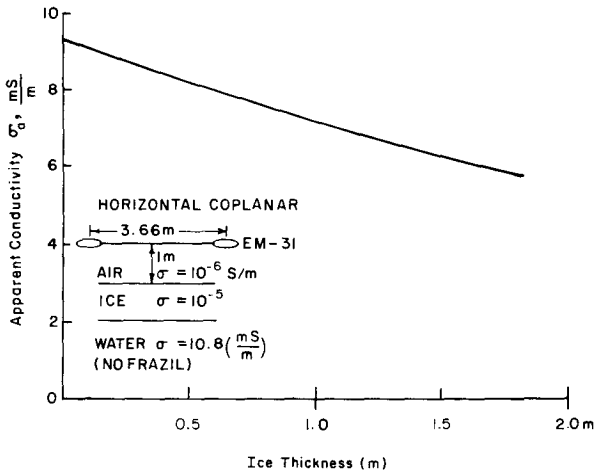

Figure 2. Calibration curve for an EM31 instrument held at 1-m height above an ice sheet of varying thickness and a deep water layer.

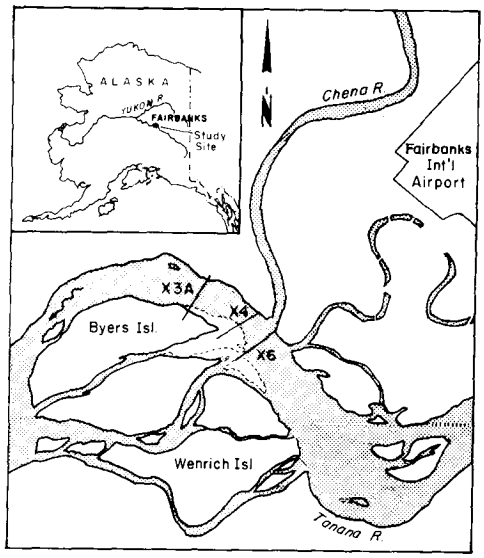

Figure 3. Location of the study site on the Tanana River, near Fairbanks, Alaska. Cross sections of lines X6, X4, and X3A were the 3 of 27 transects that were measured and compared to MI data.

lished by Geonics Ltd. (App. B) in their operation manual and based on the work of Sinha (1976). Generally, the instrument in the HCP mode is sensitive to a depth of about two times the intercoil spacing or 7 m. Its lateral sensitivity is about equal to the intercoil spacing. The VCP mode is less sensitive to depth. Arcone et al. (1979) discuss this more fully and use a thin conductive layer at depth to demonstrate depth sensitivity theoretically. The HCP mode was chosen because we expected frazil deposits to 6 m depth and also wanted to sense bottom sediments.

MI is most accurate for conductivities greater than 1 mS/m and least accurate for conductivities less than 0.05 mS/m . This loss in accuracy results from the difficulty in obtaining a site of extremely low conductivity at which a correct zero point ($\sigma = 0$) calibration can be made. In these studies, we expected a wide range of values due to the general four-layer system of ice, water, frazil ice, and bottom sediment, the total depth of which was within the general sensitivity range of this instrument. Figure 2 shows the calibration curve for solid ice ($\sigma < 10^{-5}$ S/m) above Tanana River water (0.011 S/m) and gives values between 6 and 9 mS/m for ice of varying thickness over water deeper than about 6 m. Values less than 6 mS/m would be expected to have been influenced by either frazil ice or bottom sediments.

SITE DESCRIPTION AND SURVEY METHODS

The study area is located at the confluence of the Chena and Tanana Rivers, just south of Fairbanks International Airport (Fig. 3). The active floodplain of the Tanana River in the study area is approximately 500 m wide, with total water depth ranging from 11 m in the main channel along the north shore to about 2 m over some mid-channel bars. MI apparent conductivity and ground truth data were measured along three cross sections (X3A, X4 and X6) as well as along 24 additional transects for which ground truth was not obtained. The EM31 was hand-held at the operator's hip in the HCP mode with the instrument axis perpendicular to the transects. Readings were taken every 2 m and typically 30 minutes were required to complete each profile.

Hydrographic cross sections of X3A, X4, and X6 were constructed from data measured in access holes augered every 10 m along each cross section. These data included ice cover thickness, frazil deposit thickness, and water depth. Snow depth was also recorded to position the instrument accurately above the ice cover. Data for the frazil deposits describe only particle size and sediment concentration and did not record volumetric water content, which was estimated to be as high as 60%. A typi-

cal well log description is given by Chacho et al. (1986). Water conductivity was measured at 0.011 S/m using a YSI conductivity meter in the field.

CROSS SECTION FIELD DATA AND MODELING RESULTS

The theory used to develop the model assumes homogeneous, laterally infinite layers, each characterized by one conductivity and the thickness recorded in the well log. In other words, at each observation point each material (frazil ice, solid ice, water, or sediment) is idealized as being of infinite lateral extent. This is a fairly good assumption considering the large vertical-to-horizontal scale (aspect ratio of ~ 20:1) distortions used in the cross sections and in light of the fact that the instrument is sensitive mainly to a lateral distance r from the center of the instrument (Arcone et al. 1979). The modeling also accounts for the height at which the instrument was held. Conductivity values for air, snow (0 to 35 cm), and solid ice were assumed 10^{-5} S/m; any smaller value does not affect the results. Conductivity values for the frazil ice and river bed were derived by trial and error for cross section X6 and then applied to X3A and X4.

All field data were gathered on 1 and 2 March 1986, when air temperature never exceeded −2°F. This fact and the diagreement between measured and theoretical values over the deep water channels on cross section X4 suggest that we may, at times, have experienced operating difficulties with the EM31. Sources of error are discussed in Appendix A.

X6

The measured cross section is compared with measured (solid curve) and hypothetically modeled (broken curves) MI conductivity profiles in Figure 4. The highest measured conductivity values occurred over the deepest water channels beneath the ice cover, while the lowest values were measured on the north bank of frozen silt and over the ice-covered gravel bar at the southern end of the cross section. A large minimum occurred between 50 and 80 m, above the frazil deposit. A secondary minimum occurred at about 125 m, over a small, hanging frazil deposit.

A value of 1.0×10^{-3} S/m was derived for the river bed by modeling the MI response at points A and C. This value was then applied at point B to derive a value of 6.3×10^{-4} S/m for the frazil ice deposit. Ground conductivity values calculated or measured are given in Figure 4 and were used to

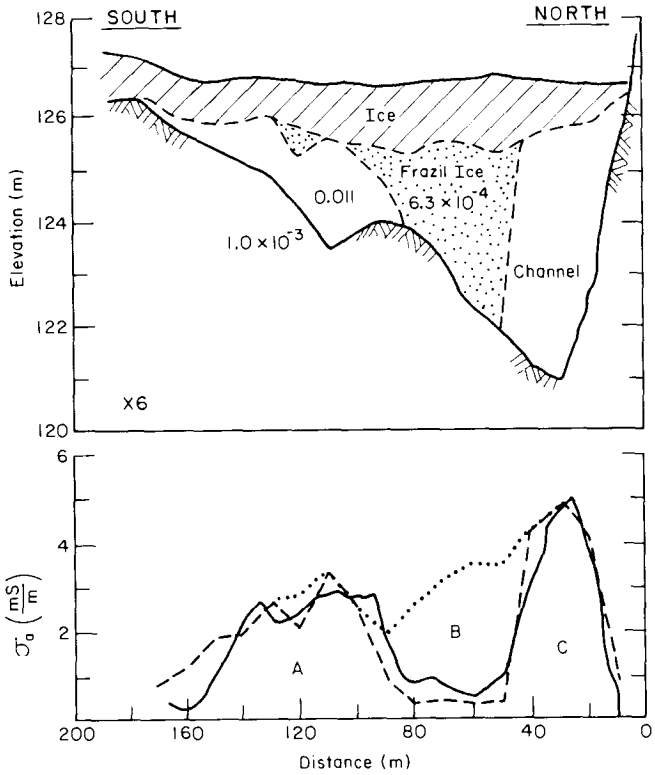

Figure 4. Comparison of measured EM31 data for cross section X6 (solid line) with a theoretical model (dashed line). Conductivity values (S/m) for the model: ice = 10^{-5} (assumed), water = 0.011 (measured), bottom sediments = 10^{-3}, and frazil ice deposits = 6.3×10^{-4}. The sediment and frazil values were derived by trial and error from data at points A, B, and C. The dotted curve is the theoretical response if the frazil ice deposits were replaced by water. A comparison of the two broken curves demonstrates the sensitivity of the MI technique to the presence of the frazil deposits.

produce the theoretical dashed curve, which correlates well with the measured curve. The dotted curve of Figure 4 gives the theoretical response when water is substituted for the frazil ice. It is apparent from the comparison of the broken curves here and in the figures that follow that the instrument is sensitive to the presence of the frazil ice deposits. This sensitivity reflects the low conductivity of these deposits, which is surprising in view of the large amount of unfrozen interstitial water that was observed. Theoretical mixing formulas (e.g. Fricke 1924) suggest that ice-water mixtures of high volumetric ice content should be an order of magnitude greater in conductivity. However, these formulations assume structures with high electrical permeability, which may not be true here.

X3A

The cross sections and conductivity profiles for X3A are given in Figure 5. As in Figure 4, the solid curve on the bottom graph gives the measured data, the dashed curve gives the model data, and the dotted curve gives model data with frazil ice replaced by water. Conductivity values for the bottom sediment and frazil deposits are the same as used for line X6. As in line X6, maximum conductivity values occur over the open water sections and minima occur where frazil ice exists to the river bottom. The modeled and observed data agree excellently up to 120 m, especially over the water channels where there are changes in σ_a due to changes in both solid ice and water depths. Between 120 and 180 m the agreement is mainly qualitative as there are apparently more changes occurring than were found by drilling. Assuming that the value 1.0 mS/m is still correct for the bottom sediments in this section, the frazil ice conductivity would have to be raised to about 7 mS/m to given more reasonable quantitative correlation between measured and modeled data in this section. This suggests that the electrical permeability in this section of frazil ice was greater than in other sections.

X4

The observed and modeled data for X4 are given in Figure 6. There is good reason to believe that the instrument was operating incorrectly for this profile as there is less quantitative agreement between observations and theory than before over most of the profile, especially over the main channel. The error is apparently an offset of about 1 mS/m, which seems less between 60 and 95 m because the instrument does not measure below 0 mS/m. Nevertheless, the qualitative agreement is good as maxima in the profile occur only over the open water sections. The maximum seen in σ_a in

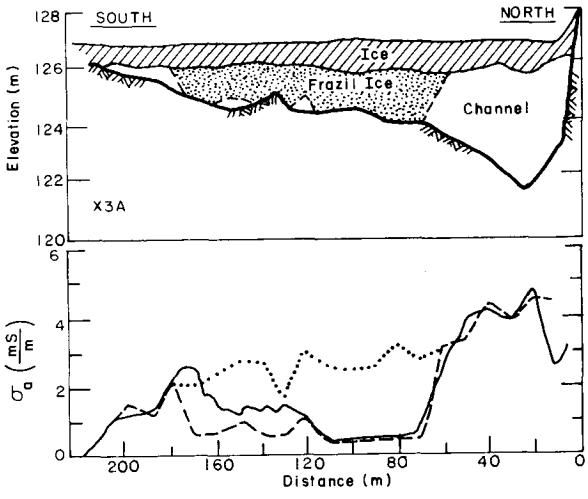

Figure 5. Comparison of measured EM31 data for cross section X3A (solid line) with a theoretical model (dashed line).

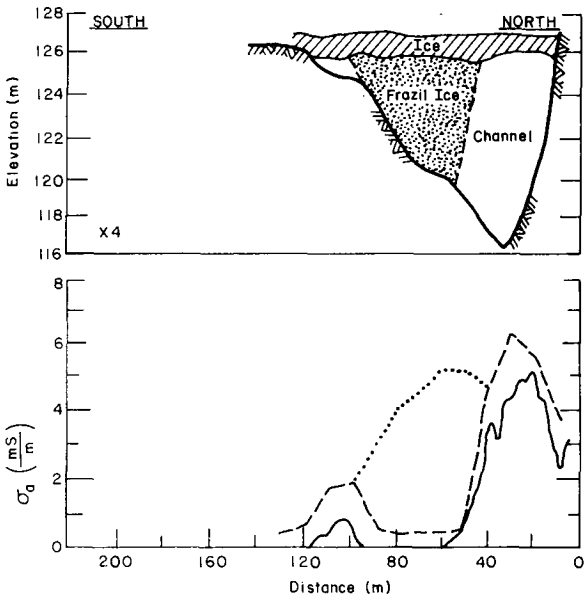

Figure 6. Comparison of measured EM31 data for cross section X4 (solid line) with a theoretical model (dashed line).

the dotted profile from 50 to 60 m is due to a dramatic decrease in the thickness of the ice cover between the 40- and 50-m stations (see Appendix B, Table B3), thus allowing the more conductive water to be closer to the instrument.

CONCLUSIONS AND RECOMMENDATIONS

The conductivity of the frazil deposits usually contrasted well with the conductivities of the river water and the solid ice cover, but the conductivity of the gravels or gravelly sand at the bottom of the Tanana were comparable to that of the frazil ice. Thus, the major obstacle to magnetic induction frazil detection would be shallow streams where bottom sediments could be confused with frazil ice. Conductivity values far below those expected for solid ice over water would be a significant indication of frazil ice deposits, if water depth were known to be much deeper than the penetration depth of the instrument. Frazil deposits with high volumetric water contents will be more conductive and less detectable. Therefore the MI method would apply primarily to dams or deposits with low water content.

Any one vertical cut in a cross section can have as many as four different layer thicknesses and five different conductivities. The thickness of the ice, frazil ice, and water and the conductivities of the frazil and bottom sediments would all be unknown. Therefore, the use of the MI technique (without drilling) to resolve all these parameters requires a multimode operation in which either the loop orientation, frequency, and/or coil separation is varied. Use of one instrument in the vertical coplanar (VCP) mode as well as the HCP mode would increase sensitivity to frazil deposits but generally decrease sensitivity to depth. The use of two MI instruments with different coil spacings would supply four pieces of information, enough to solve theoretically for the truly unknown parameters solid ice depth, frazil ice or water depth, frazil ice conductivity, and bottom sediment conductivity, assuming either water or frazil ice exists at any point beneath the solid ice cover, but not both. Thickness of the ice cover can be measured separately with GPR using pulses centered above 500 MHz, which has demonstrated sensitivity to solid ice depth, but not to frazil deposits with high water content (Arcone and Delaney, in prep.).

LITERATURE CITED

Arcone, S.A. (1985) Radar profiling of ice thickness. USA Cold Regions Research and Engineering Laboratory, Cold Regions Technical Digest No. 85-1.

Arcone, S. and A. Delaney (In preparation) Airborne river ice thickness profiling with helicopter-borne UHF short pulse radar. *Journal of Glaciology.*

Arcone, S.A., P.V. Sellmann and A.J. Delaney (1978) Shallow electromagnetic investigations of permafrost. In *Proceedings of the Third International Conference on Permafrost, July 10–13, 1978, Edmonton, Alberta, Canada.* Vol. 2. Ottawa: National Research Council of Canada, p. 501–507.

Arcone, S.A., P.V. Sellmann and A.J. Delaney (1979) Effects of seasonal changes and ground ice on electromagnetic surveys of permafrost. USA Cold Regions Research and Engineering Laboratory, CRREL Report 79-23.

Chacho, E.F., D.E. Lawson and B.E. Brockett (1986) Frazil ice pebbles: Frazil ice aggregates in the Tanana River near Fairbanks, Alaska. In *Proceedings, IAHR Symposium on Ice 1986, Iowa City, August 18–22, 1986.* Vol. I, p. 475–484.

Fraser, D.C. (1978) Resistivity mapping with an airborne multicoil electromagnetic system. *Geophysics,* **43**(1): 144–172.

Fricke, H. (1924) A mathematical treatment of the electric conductivity and capacity of disperse systems. I. The electric conductivity of a suspension of homogeneous spheroids. *Physical Review, Ser. 2,* **24**(5): 575–587.

Hoekstra, P. (1978) Electromagnetic methods for mapping shallow permafrost. *Geophysics,* **43**(4): 782–787.

Hoekstra, P., A. Sartorelli and S.B. Shinde (1979) Low frequency methods for measuring sea ice thickness. In *Proceedings of the International Workshop on the Remote Estimation of Sea Ice Thickness, St. John's, Newfoundland, 25–26 September 1979.* St. John's: Memorial University, C-CORE 80-5.

Keller, G.V. and F.C. Frischknecht (1966) *Electrical Methods in Geophysical Prospecting.* New York: Pergamon Press.

Lawson, D.E., E.F. Chacho, Jr., B.E. Brockett, J.L. Wuebben, C.M. Collins, S.A. Arcone and A.J. Delaney (1986a) Morphology, hydraulics and sediment transport of an ice-covered river: Field

techniques and initial data. USA Cold Regions Research and Engineering Laboratory, CRREL Report 86-11.

Lawson, D.E., E.F. Chacho, Jr. and B.E. Brockett (1986b) Sub-ice channels and longitudinal frazil bars, ice-covered Tanana River, Alaska. In *Proceedings, IAHR Symposium on Ice 1986, Iowa City, August 18–22, 1986.* Vol. I, p. 465–474.

Sinha, A.K. (1976) Determination of ground constants of permafrost terrains by an electromagnetic method. *Canadian Journal of Earth Sciences,* **13**: 429.

APPENDIX A: DISCUSSION OF ERRORS

The sources of error associated with the MI method include internal system errors and external noise errors. System errors include offset error due to incorrect calibration and zero position drift due to temperature changes. Noise errors mean responses to extraneous electric or magnetic fields (coherent or random) generated by artificial or natural sources. Inaccurate estimates of layer conductivities will obviously bias any modeling attempt at interpretation.

Offset errors are nullified by calibrating the zero position of the meter over an area of known, low conductivity, preferably less than 10^{-4} S/m. This procedure was repeated several times during these surveys. Zero position drift is specified by the manufacturer to be about 10^{-4} S/m per 10°C change in temperature for the quadrature phase component. This is a minute correction and the manufacturer claims reliable operation to −40°C. All surveys were performed 1 and 2 March 1986, during which time temperatures ranged between −2 and −35°F. The meter contains a battery check mode, which always indicated proper function. Some readings made on land during this time proved inconsistent, so that changing water or bottom sediment conductivity are not believed to be a possible cause for the difference in response levels between line X4 and the other two. Problems related to temperature are therefore still suspect, possibly in the metering system, as discussed below.

Errors due to magnetic fields generated by telluric currents are possible in the Arctic due to worldwide thunderstorm (sferics) or by auroral activity. The maximum magnetic flux density generated by the instrument transmitter (a coil of 200 turns and current moment of about 1 amp-m^2) is about 4×10^{-7} Tesla, a value easily exceeded by natural fields. However, it is doubtful that sufficient field strength exists at 39 kHz to warrant serious consideration of telluric or auroral activity, which is generally confined to frequencies less than 10 Hz. No power lines or underground cables were remotely near the study site. The most plausible explanation is error due to static electric fields generated by inadvertent hand contact on the meter window. This problem only arises in very cold temperatures when it is easily induced by rubbing the window. Leakage of such charge appears to be slow. The best solution is to utilize a digital readout system (connected to a data logger), which has recently become available from the same manufacturer.

APPENDIX B: MODELING DATA

The following tables give the material thicknesses used to model the EM31 data. An additional (estimated) 91 cm was added to the snow thickness to account for the operating height of the instrument. The values obtained are for the horizontal coplanar (HCP) mode, which is also referred to in the literature as the vertical magnetic dipole (VMD) mode. The equation used for computing apparent conductivity σ_a is as follows:

$$\sigma_a = \sigma_1[1 - R(z_1)] + \sigma_2[R(z_1) - R(z_2)] + \sigma_3[R(z_2) - R(z_3)] + \ldots \quad \text{(B1)}$$

where

$$R(z_n) = 1\sqrt{(2z_n/r)^2 + 1} \qquad n = 1,2,3\ldots. \quad \text{(B2)}$$

The quantities σ_n are the successive conductivities of the layers, z_n the depths from the surface to each of the layer interfaces, and r the intercoil spacing, which is 3.66 m for the EM31. This layering theory may be applied where the extent of the layering beneath the point of measurement extends at least over an area whose radius $\cong r$.

Table B1. Snow, ice, and water layer thicknesses used in eq B1 to derive the EM31 conductivity values (columns 6, 7) for line X6.

Dist (m)	Snow* (cm)	Solid ice (cm)	Frazil (cm)	Water (cm)	EM31 (mS/m)	Frazil replaced by water (mS/m)
10	15	30	--	--	0.80	
15	15	41	--	142	3.22	
20	15	81	--	307	4.22	
30	15	91	--	490	4.89	
40	15	124	--	442	4.20	
50	15	150	353	--	0.47	3.51
60	15	124	315	--	0.51	3.65
70	15	117	231	--	0.54	3.23
80	15	135	152	--	0.54	2.43
90	15	112	61	36	0.98	1.87
100	15	112	--	163	2.50	
110	15	97	--	213	3.34	
120	15	71	51	91	1.97	2.92
130	15	71	--	112	2.55	
140	15	84	--	66	1.81	
150	15	94	--	69	1.79	
160	15	76	--	23	1.14	
170	15	81	--	8	0.84	

*Not recorded. Values in this table are the average for all other lines.

Table B2. Snow, ice, and water layer thicknesses used in eq B1 to derive the EM31 conductivity values (columns 6, 7) for line X3A.

Dist (m)	Snow (cm)	Solid ice (cm)	Frazil (cm)	Water (cm)	EM31 (mS/m)	Frazil replaced by water (mS/m)
15	8	71	--	320	4.56	
20	5	79	--	335	4.57	
30	2	124	--	386	3.95	
40	1	79	--	323	4.37	
50	2	102	--	244	3.51	
60	1	112	--	201	3.09	
70	10	112	170	--	0.57	2.86
80	3	99	183	--	0.60	3.19
90	10	117	155	--	0.57	2.69
100	1	122	122	--	0.57	2.27
110	23	107	155	--	0.57	2.66
120	23	79	122	43	1.09	3.01
130	30	79	71	--	0.63	1.83
140	28	69	145	--	0.62	2.85
150	25	79	119	33	0.99	2.86
160	23	91	124	--	0.60	2.46
170	30	84	99	--	0.61	2.16
180	20	71	--	81	2.09	
190	18	91	--	33	1.28	
200	23	64	--	48	1.60	
210	25	76	--	1	0.71	

Table B3. Snow, ice, and water layer thicknesses used in eq B1 to derive the EM31 conductivity values (columns 6, 7) for line X4.

Dist (m)	Snow (cm)	Solid ice (cm)	Frazil (cm)	Water (cm)	EM31 (mS/m)	Frazil replaced by water (mS/m)
10	3	112	--	348	3.81	
15	28	74	--	442	4.75	
20	23	74	--	686	5.62	
30	0	84	--	922	6.30	
40	5	145	--	688	4.71	
50	5	107	579	--	0.51	5.08
60	5	102	561	--	0.51	5.11
70	15	94	541	--	0.48	4.60
80	20	122	406	--	0.49	4.03
90	20	99	185	--	0.57	3.02
100	23	117	--	97	1.95	
110	23	91	--	69	1.76	
120	23	81	--	8	0.83	
130	23	81	--	--	0.69	